



DIGITAL ACCESS TO SCHOLARSHIP AT HARVARD

X-Ray Studies of Tilted Hexatic Phases in Thin Liquid-Crystal Films

The Harvard community has made this article openly available.
[Please share](#) how this access benefits you. Your story matters.

Citation	Sirota, E. B., Peter S. Pershan, L. B. Sorensen, and J. Collett. 1985. X-ray studies of tilted hexatic phases in thin liquid-crystal films. <i>Physical Review Letter</i> 55(19): 2039–2042.
Published Version	doi:10.1103/PhysRevLett.55.2039
Accessed	February 18, 2015 11:24:19 PM EST
Citable Link	http://nrs.harvard.edu/urn-3:HUL.InstRepos:10357489
Terms of Use	This article was downloaded from Harvard University's DASH repository, and is made available under the terms and conditions applicable to Other Posted Material, as set forth at http://nrs.harvard.edu/urn-3:HUL.InstRepos:dash.current.terms-of-use#LAA

(Article begins on next page)

X-Ray Studies of Tilted Hexatic Phases in Thin Liquid-Crystal Films

E. B. Sirota and P. S. Pershan

Division of Applied Sciences, Harvard University, Cambridge, Massachusetts 02138

L. B. Sorensen

Department of Physics, University of Washington, Seattle, Washington 98195

and

J. Collett^(a)

*Division of Applied Sciences, Harvard University, Cambridge, Massachusetts 02138,
and IBM Thomas J. Watson Research Center, Yorktown Heights, New York 10598*

(Received 22 January 1985)

X-ray-diffraction studies of the structures and phase transitions of the tilted hexatic phases (smectic *F* and smectic *I*) in thin liquid-crystal films of 4-*n*-heptyloxybenzylidene-4-*n*-heptylaniline (7O.7) are reported. The measured correlation lengths were strongly anisotropic in both phases. The smectic-*I* to smectic-*F* transition is first order as expected from the symmetry change. The smectic-*F* to smectic-*G* transition is first order with strong pretransition effects and becomes nearly second order as the film thickness is decreased.

PACS numbers: 64.70.-p, 61.30.-v

There is currently great interest in the hexatic phases of matter. The hexatic phases have order intermediate between that of liquids and solids, with liquid-like short-range order of the in-plane positional correlations and solidlike quasi long-range order [in two dimensions (2D)] or long-range order [in three dimensions (3D)] of the orientation of the geometric bonds connecting the in-plane neighboring molecules.¹ Liquid-crystal systems provide ideal samples to study these remarkable phases because they have an extremely weak interlayer coupling which allows these materials to exhibit 3D stacked hexatic phases in addition to the standard 2D phases.² There are three different 3D smectic hexatic phases³: one untilted hexatic (hexatic *B*) and two tilted hexatics (smectic *F* and smectic *I*). Although most of the experimental studies of the liquid-crystal hexatic phases have concentrated on the structure of the hexatic-*B* phase and on the hexatic-to-liquid phase transition (hexatic *B* to smectic *A*)⁴ there have been a few basic studies of similar phenomena in tilted systems.⁵⁻¹⁰ In this Letter we report the first systematic x-ray-scattering study of the temperature dependence and anisotropy of the correlation lengths in the two tilted hexatic phases.

In freely suspended films of 4-*n*-heptyloxybenzylidene-4-*n*-heptylaniline (7O.7) the smectic-*F* (Sm*F*) and the smectic-*I* (Sm*I*) phases only occur for films thinner than approximately 280 and 25 layers, respectively.¹¹ We also report similar anisotropies in the Sm*F* phase of thick films of two homologous compounds, 5O.6 and 9O.4, suggesting that the anisotropy is a universal feature of the tilted hexatics. Since the observed positions of the diffuse peaks in the Sm*F* phase and the Bragg peaks in the crystalline-*G* (Cr*G*)

phase are essentially coincident, this is an explicit demonstration that the short-range structure is identical in these two phases and thereby establishes that the hexatic Sm*F* phase is a faulted version of the Cr*G* phase.⁶

The high-resolution x-ray-diffraction studies were carried out on the triple-axis spectrometer installed on beam line VII-2 at the Stanford Synchrotron Radiation Laboratory (SSRL).¹² A pair of asymmetrically cut Ge[111] crystals were used in the double-crystal monochromator and a single LiF[200] crystal was used as an analyzer; this resulted in a longitudinal resolution of $\Delta Q = 3.8 \times 10^{-3} \text{ \AA}^{-1}$. The low-resolution measurements were made with a rotating-anode source of Cu *K* α radiation and a triple-axis spectrometer at Harvard University. The monochromator was a vertically focusing pyrolytic graphite [002] crystal and the analyzer was a flat pyrolytic graphite [002] crystal; this resulted in a longitudinal resolution of $\Delta Q = 5 \times 10^{-2} \text{ \AA}^{-1}$.¹³ The freely suspended films were drawn across a 7-mm-diam aperture in an oven which has been described in detail elsewhere¹⁴; the pressure inside the oven was maintained at 1 Torr and the temperature was regulated to ± 5 mK. The films were oriented with the normal to the smectic layers always in the scattering plane. Scans were done along Q_{xy} , parallel to the planes of the smectic layers, or along Q_z , normal to the layers. A rotation stage inside the oven allowed rotation about an axis normal to the smectic layers thereby varying the direction of Q_{xy} within the smectic layers.

The phase diagram for 7O.7 is shown in Fig. 1 as a function of both temperature and film thickness. For thicknesses greater than ~ 280 layers, the structures

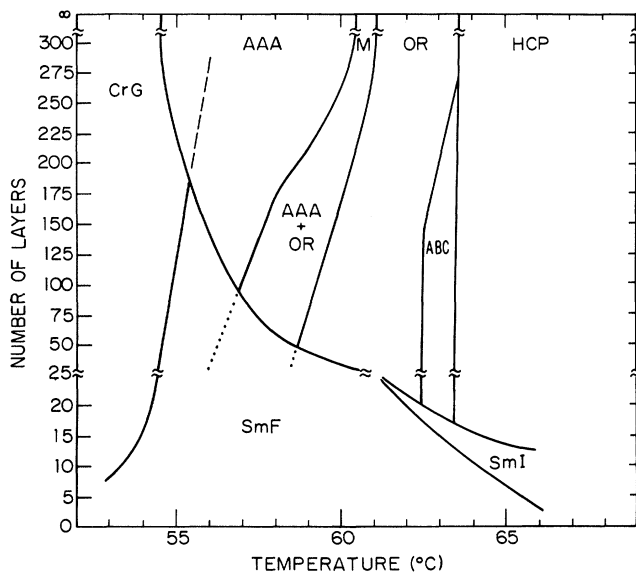


FIG. 1. Thickness vs temperature phase diagram for 70.7. The solid lines indicate the reversible phase boundaries; the dashed (dotted) lines indicate boundaries of unstable phases observed kinetically on heating (cooling). The phases are crystalline *G* (CrG), smectic *F* (SmF), smectic *I* (SmI), hexagonal *AAA* (*AAA*), orthorhombic (OR), hexagonal *ABC* (*ABC*), hexagonal close packed (hcp), and monoclinic (M).

of the various crystalline phases and their respective phase transitions have been described elsewhere.^{11,14-16} The crystalline-*B* (CrB) phase between ~ 69 and 63.5°C is a hexagonal close-packed lattice with *ABAB* stacking and two molecules per primitive unit cell. At 63.5°C there is a first-order dislocation-mediated transition to a lattice in which the local stacking is *ABC* with one molecule per primitive unit cell.¹⁶ For thick samples, the dislocations interact to form regular arrays of low-angle grain boundaries that result in a modulated structure with orthorhombic macroscopic symmetry. At slightly lower temperatures there are further transitions to phases that are still locally *ABC* but with macroscopic symmetries that are first monoclinic (61°C) and then hexagonal with *AAA* stacking (60.5°C). At $\sim 55^\circ\text{C}$ the system undergoes a first-order transition to a CrG phase in which the molecules are tilted by about 22° to the layer normal. With decreasing film thickness, starting at ~ 280 layers, the monoclinic phase is gradually replaced by a coexistence between the orthorhombic and the *AAA* phases. In addition, the direct first-order transition from the *ABAB* to the orthorhombic phase is replaced by a region in which the orthorhombic phase coexists with a hexagonal phase with macroscopic *ABC* stacking.

The most surprising change in the phase diagram¹¹ is the inclusion of two tilted hexatic phases (SmF and

SmI) which do not appear in bulk 70.7. The SmF phase starts appearing as a reversible intervening phase between the *AAA* and the CrG phases when the film thickness is reduced below about 180 layers. However, when we heat (films with thickness between 180 and 280 layers) from the CrG phase to the *AAA* phase, a kinetic CrG-*AAA* coexistence gives way to a kinetic SmF-*AAA* coexistence along the dashed line in Fig. 1. The SmI phase first appears at a film thickness of about 25 layers. When the SmF and the SmI phases first appear they exist only over narrow temperature ranges, but as the thickness is reduced further, these ranges increase substantially. Because the phase diagram is so rich, a wide variety of phase transitions can be studied by variation of the temperature at a fixed film thickness. These transitions include several solid-to-hexatic transitions (*AAA* to SmF, orthorhombic to SmF, *ABC* to SmI, and hcp to SmI), a hexatic-to-hexatic transition (SmI to SmF), and a hexatic-to-solid transition (SmF to CrG). All of these transitions, except for the SmF-to-CrG transition, are expected to be first order because of the change in symmetry across the transition and they were all observed to be first order. The SmF-to-CrG transition is allowed by symmetry to be a second-order transition and, as discussed below, appeared to become more nearly second order as the film thickness was decreased.

High-resolution measurements of the in-plane and the interlayer correlations were made at SSRL for a series of thirteen-layer films [see Figs. 2(a) and 2(b)]. The in-plane correlation lengths are proportional to the reciprocals of the half widths at half maxima (HWHM) of the appropriate longitudinal (Q_{xy}) scans, and the interlayer lengths are similarly related to the HWHM of the transverse (Q_z) scans. In view of the fact that the films were composed of many domains, providing only a partial χ average, we did not attempt detailed fits to theoretical line shapes. The molecular tilt distorts the in-plane hexagonal structure sufficiently that the instrumental resolution in the in-plane direction allowed us to characterize the anisotropic correlations in the SmF phase. In the CrG phase each layer consists of a hexagonal 2D lattice which is slightly distorted by the molecular tilt, which results in a centered rectangular lattice. This produces two inequivalent in-plane reciprocal-lattice vectors $(Q_{xy})_1 = 0.925(4\pi/\sqrt{3}a)$ and $(Q_{xy})_2 = 0.98(4\pi/\sqrt{3}a)$, where a is the hexagonal lattice parameter in the CrB phases; $a = 5.05 \text{ \AA}$. Since the molecular tilt of 22° from the layer normal is accompanied by lateral displacements of adjacent layers the Bragg peaks are also displaced along Q_z . Together these effects result in Bragg peaks at $(Q_z)_1 = 2.6(2\pi/l)$ and $(Q_z)_2 = 1.3(2\pi/l)$, where the molecular length is $l = 30.6 \text{ \AA}$. The corresponding Q_{xy} and Q_z scans are resolution limited in the CrG phase. On heating into

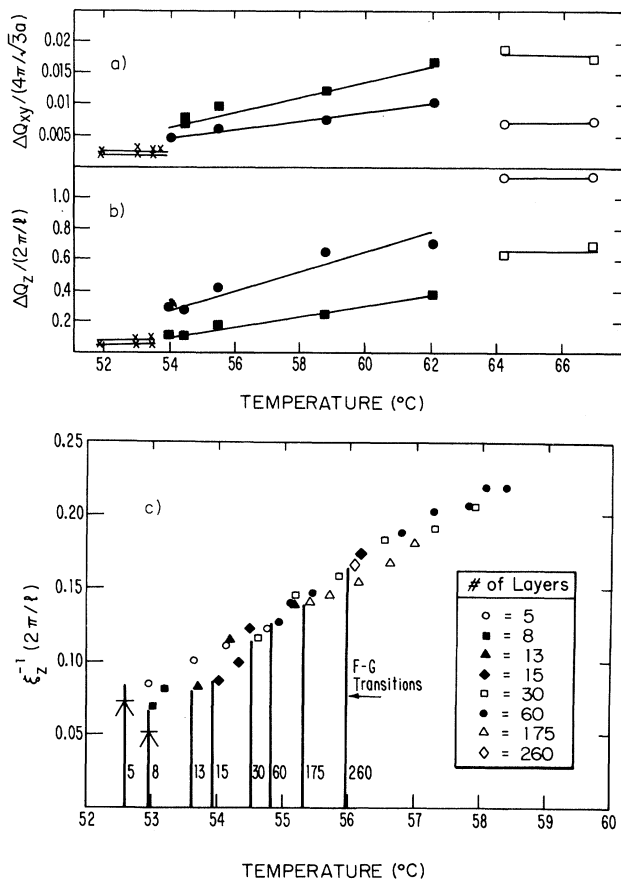


FIG. 2. The temperature dependence of the measured linewidths in the crystalline-*G* (Cr*G*), smectic-*F* (Sm*F*), and smectic-*I* (Sm*I*) phases of 7O.7. (a) High-resolution measurements illustrating the in-plane anisotropic linewidths (HWHM) of Q_{xy} scans for a thirteen-layer film at SSRL. Sm*I* phase: open circles, $(Q_z)_2/(2\pi/l)=0$; open squares, $(Q_z)_1/(2\pi/l)=2.0$. Sm*F* phase: solid circles, $(Q_z)_2/(2\pi/l)=1.3$; solid squares, $(Q_z)_1/(2\pi/l)=2.6$. The crosses indicate the instrumental resolution measured in the Sm*G* phase. The solid lines are guides for the eye. The units are $4\pi/\sqrt{3}a=1.436 \text{ \AA}^{-1}$ and $2\pi/l=0.205 \text{ \AA}^{-1}$. (b) High-resolution measured linewidths (HWHM) illustrating the interlayer anisotropy observed in the Q_z scans for a thirteen-layer film at SSRL. Sm*I* phase: open circles, $(Q_{xy})_2=0.988(4\pi/\sqrt{3}a)$; open squares, $(Q_{xy})_1=0.955(4\pi/\sqrt{3}a)$. Sm*F* phase: solid circles, $(Q_{xy})_2=0.975(4\pi/\sqrt{3}a)$; solid squares, $(Q_{xy})_1=0.927(4\pi/\sqrt{3}a)$. The crosses indicate the mosaic limit measured in the Sm*G* phase. The solid lines are guides for the eye. The units are as above. (c) Fitted reciprocal correlation lengths from low-resolution measurements of the temperature dependence of the observed Q_z linewidths for the Sm*F* phase of 7O.7 as a function of the film thickness, n . For each thickness, the measurements followed a single universal curve until they underwent the first-order jump (indicated by the solid bar) at their respective Sm*F*-to-Cr*G* transitions. The arrows indicate the finite-size limits for the 5 to 8 layer films.

the Sm*F* phase the resulting diffuse peaks remain at the same positions which demonstrates that the Sm*F* phase has the same short-range order as the Cr*G* phase. The observed widths are shown in Figs. 2(a) and 2(b). The decrease in HWHM with decreasing temperature indicates increased interlayer and intralayer correlations. Budai *et al.* observed a similar trend in the Sm*I* phase of a different material.⁹

The interlayer correlations in the Sm*F* phase were studied as a function of the film thickness by use of the low-resolution spectrometer at Harvard. With this spectrometer, nearly complete χ averages were practical so that the measured line shapes could be fitted to obtain the temperature dependence of the correlations [Fig. 2(c)]. For films ranging in thickness from 8 to 260 layers the temperature dependence observed was found to be identical to that observed for the thirteen-layer films at SSRL. For all of the thicknesses measured, the observed linewidths fall on a single universal curve with the observed first-order jump at the Sm*F*-to-Cr*G* transition becoming smaller as the film thickness (and the Sm*F*-to-Cr*G* transition temperature) decreased. The observed correlation lengths appear to be independent of both the film thickness and the temperature range of the Sm*F* phase and to depend only on the absolute temperature. This suggests that although the Sm*F* phase in 7O.7 is only observed in thin films, it is actually a stable phase that would exist in bulk were it not preempted by another phase with lower free energy. According to this model the chemical potentials of the Sm*F* and Cr*B* (*AAA*) phases in 7O.7 must be nearly equal, with the Cr*B* phase having a slightly lower value in bulk. Presumably surface-induced tilt causes the Sm*F* to have a lower chemical potential for films thinner than ~ 180 layers. This observation is clear evidence for the idea that the near equality of the chemical potentials for various ordered phases is responsible for the variety of phase sequences for closely related chemical homologs. We plan to study the behavior of two-layer films to see if the trend toward a second-order transition continues.

Anisotropic correlations were also observed in the Sm*F* phases of the homologous compounds, 5O.6 and 9O.4, with use of a low-resolution spectrometer.¹³ The observed HWHM for 9O.4 were $(\Delta Q_z)_1=0.13 \text{ \AA}^{-1}$ and $(\Delta Q_z)_2=0.17 \text{ \AA}^{-1}$, and $(\Delta Q_{xy})_1=0.014 \text{ \AA}^{-1}$ and $(\Delta Q_{xy})_2=0.011 \text{ \AA}^{-1}$ at 68.5 °C. Only the interlayer correlations were studied for 5O.6 with the results $(\Delta Q_z)_1=0.12 \text{ \AA}^{-1}$ and $(\Delta Q_z)_2=0.18 \text{ \AA}^{-1}$ at 41.4 °C. The temperature dependence for these materials is currently under study.¹⁷ We were able to align the tilt field in the Sm*F* phase of 9O.4 producing well-aligned single-domain samples by slowly cooling from the Sm*A* into the Sm*F* phase. The sixfold hexatic order in the Sm*F* phase was measured directly by the observation of the scattering intensity as a function of

χ around the contour of maximum molecular form factor. The sixfold order was clearly visible and explicitly demonstrated the long-range bond orientational order in the tilted hexatic phase. We were not able to produce monodomain samples of 5O.6, possibly because the phase sequence of 5O.6 is CrB to SmF.

The SmI phase differs from the SmF in the orientation of the molecular tilt relative to the near-neighbor positions.^{3,7,10} In the SmI (SmF) phase the molecules tilt towards the corner (face) of the real-space hexagon formed by the local in-plane packing. The transition from the SmF to the SmI phase is clearly first order [see Figs. 2(a) and 2(b)], as expected from the symmetry change between the phases. The principal peak positions in the SmI phase are $(Q_{xy})_1 = 0.955(4\pi/\sqrt{3}a)$, $(Q_z)_1 = 2.0(2\pi/l)$, $(Q_{xy})_2 = 0.988(4\pi/\sqrt{3}a)$, and $(Q_z)_2 = 0$ and the correlation lengths do not appear to be temperature dependent.

This study has revealed the underlying anisotropy of the tilted hexatic phases and the amazing richness of the thickness-dependent phase diagram. The spontaneous appearance of the tilted hexatic phases in thin 7O.7 films and the trend towards a second-order transition for very thin films is strongly reminiscent of the behavior of the hexatic phases predicted by the theory of 2D melting.^{18,19} In particular, the decreasing SmF-to-CrG transition temperature with decreasing thickness appears to be an example of the suppression of the melting temperature expected to be associated with reduced dimensionality.¹ Further studies of the 3D to 2D crossover in these systems are in progress and promise to enhance greatly our understanding of these remarkable phases.

This work was supported by the National Science Foundation under Grants No. DMR 82-12189 and No. DMR 80-20247. Part of this work was done at the Stanford Synchrotron Radiation Laboratory, which is supported by the U.S. Department of Energy, Office of Basic Energy Sciences. We would like to thank the staff at SSRL, especially T. Troxel, for their assistance. Conversations with D. R. Nelson are acknowledged.

^(a)Present address: Department 242/040-2, IBM, Roches-

ter, Minn. 55901.

¹For a review see D. R. Nelson, in *Phase Transitions and Critical Phenomena*, edited by C. Domb and M. S. Green (Academic, New York, 1983), Vol. 7, p. 1.

²R. J. Birgeneau and J. D. Litster, *J. Phys. (Paris)*, Lett. **9**, L399 (1978).

³G. W. Gray and J. W. Goodby, *Smectic Liquid Crystals—Textures and Structures* (Heyden, Philadelphia, 1984), pp. 153–154.

⁴S. C. Davey, J. Budai, J. W. Goodby, R. Pindak, and D. E. Moncton, *Phys. Rev. Lett.* **53**, 2129 (1984); R. Pindak, D. E. Moncton, S. C. Davey, and J. W. Goodby, *Phys. Rev. Lett.* **46**, 1135 (1981); C. C. Huang, J. M. Viner, R. Pindak, and J. W. Goodby, *Phys. Rev. Lett.* **46**, 1289 (1981).

⁵F. Moussa, J. J. Benattar, and C. William, *Mol. Cryst. Liq. Cryst.* **99**, 145 (1983).

⁶J. J. Benattar, J. Doucet, M. Lambert, and A. M. Levelut, *Phys. Rev. A* **20**, 2505 (1979).

⁷J. J. Benattar, F. Moussa, M. Lambert, and C. Germain, *J. Phys. (Paris)*, Lett. **42**, L67 (1981).

⁸A. J. Leadbetter, J. P. Gaushan, B. Kelly, G. W. Gray, and J. W. Goodby, *J. Phys. (Paris)*, Colloq. **40**, C3-178 (1979).

⁹J. Budai, R. Pindak, S. C. Davey, and J. W. Goodby, *J. Phys. (Paris)*, Lett. **45**, L1053 (1984).

¹⁰J. Doucet, P. Keller, A. M. Levelut, and P. Porquet, *J. Phys. (Paris)* **39**, 548 (1978).

¹¹J. Collett, P. S. Pershan, E. B. Sirota, and L. B. Sorensen, *Phys. Rev. Lett.* **52**, 356 (1984), and **52**, 2190(E) (1984).

¹²D. E. Moncton and G. S. Brown, *Nucl. Instrum. Methods* **208**, 579 (1983).

¹³The measurements on 5O.6 and 9O.4 were done with a position-sensitive detector rather than a crystal analyzer.

¹⁴J. Collett, L. B. Sorensen, P. S. Pershan, and J. Als-Nielsen, *Phys. Rev. A* **32**, 1036 (1985).

¹⁵J. Collett, L. B. Sorensen, P. S. Pershan, J. D. Litster, R. J. Birgeneau, and J. Als-Nielsen, *Phys. Rev. Lett.* **49**, 553 (1982).

¹⁶J. P. Hirth, P. S. Pershan, J. Collett, E. Sirota, and L. B. Sorensen, *Phys. Rev. Lett.* **53**, 473 (1984).

¹⁷E. B. Sirota and P. S. Pershan, to be published. Recent measurements show the temperature and thickness dependence of the SmF-to-CrG transition in 9O.4 to be qualitatively the same as for 7O.7.

¹⁸D. R. Nelson and B. I. Halperin, *Phys. Rev. B* **21**, 5312 (1980).

¹⁹R. Bruinsma and D. R. Nelson, *Phys. Rev. B* **23**, 402 (1981).